AADE-19-NTCE-016

Improving Drilling Reliability Through Fast Time Domain Analysis

Kaimin Yue and Raju Gandikota, MindMesh Inc.

Abstract

Advances in drilling technology enable oil & gas industry to drill faster and to minimize Non-Productive Time (NPT). This usually requires minimizing changes to the Bottom Hole Assembly (BHA) and improving its reliability. However, drilling systems are commonly subjected to dynamic dysfunctions, that can cause downhole tool failure, increase drilling cost and NPT, and compromise the wellbore quality. Therefore, understanding drilling dynamics behavior of BHA is a crucial step to improve drilling efficiency and to reduce NPT.

This study presents a fast running Time Domain Analysis (TDA) method to model drilling dysfunctions, which is based on the multibody dynamics solved by finite element methods. The TDA model allows exploration of the full range of BHA response under a realistic downhole condition, including the effects of weight on bit, RPM, BHA configurations, bit types, mud properties, formation properties, wellbore construction, and well trajectory. This model can realistically simulate various drilling dysfunctions including stick-slip, whirl, and dynamic lateral vibrations.

This paper also discusses a field case study to evaluate the mud motor failure due to lateral vibrations. Two BHAs were analyzed using TDA and the predicted lateral vibrations match well with the field data. The TDA models allow drilling engineers to explore the design space and operating conditions to optimize drilling performance and BHA reliability. It can not only be used to analyze post drilling job cases and explain issues observed in the field, but also can predict drilling dysfunctions before drilling and reduce NPT.

Introduction

Nowadays, most drilling analysis models are based on the assumption of static BHA, such as torque-drag, slide calculation, and directional tendencies. Or you have linear vibration models, from which you look at mode shape analysis without the effect of wellbore. That means the behavior of drill string is inferred from the mode shapes and linear dynamics, essentially looking at the frequency domain.

However, field measurements show that the response of drilling systems is more complicated than those predicted by the static or linear vibration models. The drilling systems can be subject to various types of oscillations with large amplitude, namely axial, lateral, and torsional mode of vibrations. The main cause of these vibrations include imbalance, eccentricity, the friction and contact between drill string and borehole, the initial curvature of drill string, and various nonlinear dynamics responses (Kamel and Yigit, 2014). The severe vibrations of drilling system can lead up to dynamic dysfunctions, which include stick-slip, whirl, and dynamic lateral vibrations (Tikhonov et al. 2014; Gandikota and Chennoufi, 2017; Pastusek et al. 2019). These drilling dysfunctions can cause downhole tool failure, increase drilling cost and NPT, and compromise the wellbore quality. In order to improve drilling efficiency and to reduce NPT in a more efficient manner, this study introduces a fast running time domain analysis (TDA) model, which can accurately and efficiently model drilling dysfunctions.

The remainder of the paper is organized as follows. In the section of models, we will discuss the time domain analysis, which is based on the multibody dynamics and finite element method. In the section of results, we will present a field case study to evaluate the motor failure due to severe lateral vibration using the time domain analysis. In the section of summaries, application of the time domain analysis and summary of results will be presented.

Models

Because of the limitations in the static and linear vibration models, several studies utilized finite element models to analyze the dynamic behavior of BHA (Oñate et al. 2012; Kamel and Yigit, 2014; Abedrabbo and Lines, 2015). But the main drawback of the FEM analysis is the intensive computational cost. In order to solve this obstacle, this study presents a Time Domain Analysis (TDA) model to analyze the nonlinear dynamic behavior of drilling systems in MindMesh's RiMo platform. The TDA model is based on the multibody dynamics, in which BHA is composed of solid bodies that are connected with each other by joints or links (Pogorelov et al. 2012; Tikhonov et al. 2013). The multibody dynamics delivers reliable solutions for various nonlinear dynamics phenomena in a fraction of time compared to FEM solutions. In addition, the nonlinear dynamics of BHA is fully coupled with the contact between the wellbore and the drill string.

Our model can not only simulate a short section of BHA but also allows the exploration of the full drilling system, from the bit to the top drive. With advanced numerical methods and

improved computing power, it allows true or near real-time capabilities to predict drilling dysfunctions. For a typical 500 feet BHA, our model usually takes several minutes to complete one-minute the time domain analysis. For a 20,000 long full range BHA, it usually takes less than one hour to complete one-minute time domain analysis.

The TDA model takes into account the detailed structures of downhole tools, such as drilling bits, mud motors, rotary steerable systems (RSS), stabilizers, and MWDs. For instance, the mud motor in our model allows the consideration of excitation due in power section, the RPM difference before and after mud motor, the bend angle, and etc. The stabilizer in the TDA model also considers the detailed description, such as number of blades, contact diameter, sleeve twist angle, and etc. In addition, densities of each downhole tools are calibrated to match the mass distribution. Furthermore, the TDA model is able to analyze the dynamics response of two types of drilling bits: PDC and Roller Cone bits. The effects of WOB, bit dimension, blade size, friction, rock strength, are considered to correctly model the nonlinear dynamical bit response. It can also realistically model the drilling dysfunctions such as stick-slip, whirl, and dynamic lateral vibrations. In addition, the TDA model can not only model the forward drilling, but also the off-bottom drilling and back reaming process.

Fig.1 shows the window for result illustration in RiMo. In the RiMo platform, we are able to plot the 2D/3D animation to illustrate the BHA dynamic vibration with/without wellbore, the time-dependent contact and lateral forces at BHA, the virtual drilling process with BHA rotating while moving in axial direction. We are also able to evaluate the time dependent drilling parameters, such as WOB, TOB, ROP, and RPM. In addition, Virtual sensors can be located anywhere along the drill string to evaluate the values of drilling dynamics parameters in any particular location: displacement, velocity, acceleration, forces, torques, and etc. RiMo also allows the user to perform data analysis easily using the implemented tools.

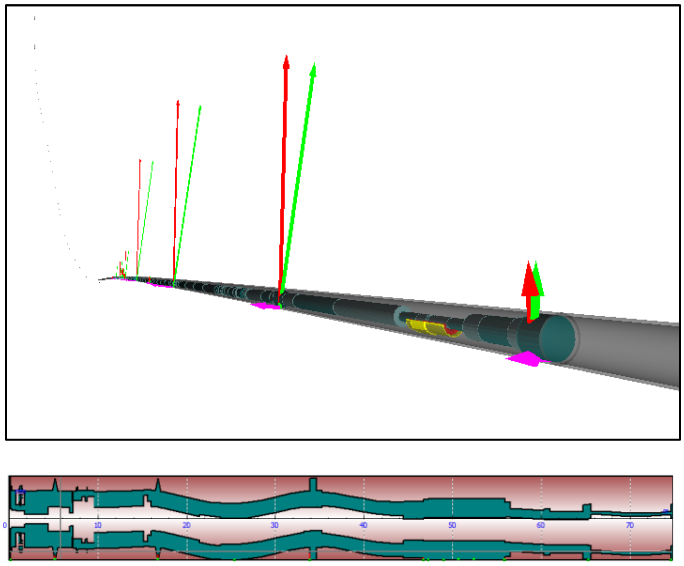

Fig. 1. 2D/3D animation of BHA dynamic vibration in RiMo. (In the 3D illustration, the red, purple, green vectors are resultant forces, normal contact forces and friction forces at the contact locations)

Results

This paper presents a field case study of utilizing the TDA model to evaluate the mud motor failure due to high lateral vibrations. One of the drilling operators found high lateral vibration as well as mud motor failure at TVD = 5520 feet when the engineers were drilling using BHA with reamer in Permian Basin. After that, they replaced the reamer with spiral stabilizer in BHA and continued drilling successfully for several thousand feet. We utilized the cutting-edge TDA model to evaluate the lateral vibrations at mud motor and to compare the difference between BHAs to optimize the design. Two types of BHA were analyzed: BHA#1 and BHA#2. BHA #1 is the new BHA that was utilized to continue drilling after 5200 feet and BHA#2 is the initial BHA that failed due to high lateral vibration at 5200 feet. Fig. 2 and Fig. 3 show the illustration of BHA#1 and BHA#2, respectively. Compared to the design of BHA#2, BHA#1 replaces the 1/8" under gauge reamer with a third spiral stabilizer and contains two more short subs below and above mud motor to measure vibrations. Both BHA#1 and BHA#2 follow the BHA setup as described in the drilling report. BHA#1 was first analyzed in our analysis to calibrate the model by comparing with vibrations measured at the downhole subs. Afterwards, BHA#2 is utilized as a comparison to understand the difference between stabilizer and reamer to optimize the BHA design.

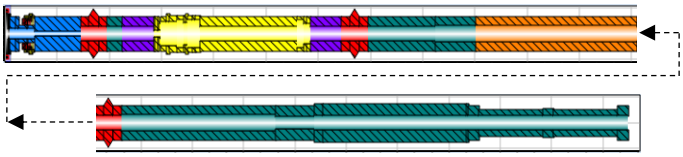

Fig. 2. Illustration of BHA #1 (The first part is bit, which is in black, the blue part is RSS, the yellow part is mud motor, the red parts are spiral stabilizers, the purple parts are data subs, and the orange part is MWD)

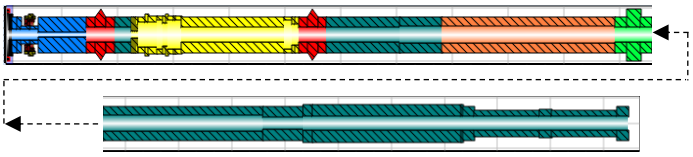

Fig. 3. Illustration of BHA #2 (The first part is bit, which is in black, the blue part is RSS, the yellow part is mud motor, the red parts are spiral stabilizers, the orange part is MWD, and the green part is roller reamer)

Fig. 4 shows the wellbore trajectory in the model, which is the same as measured in the drilling operation. To be consistent with the operation condition, the borehole diameter was considered to be 9.875 inch and the formation is considered as

limestone. At the condition of failure, the WOB is about 40 kip and the RPM of drill pipe and mud motor are 10 and 170, respectively. In order to realistically model the drilling condition, the same drilling parameters in the operation were applied in the TDA model.

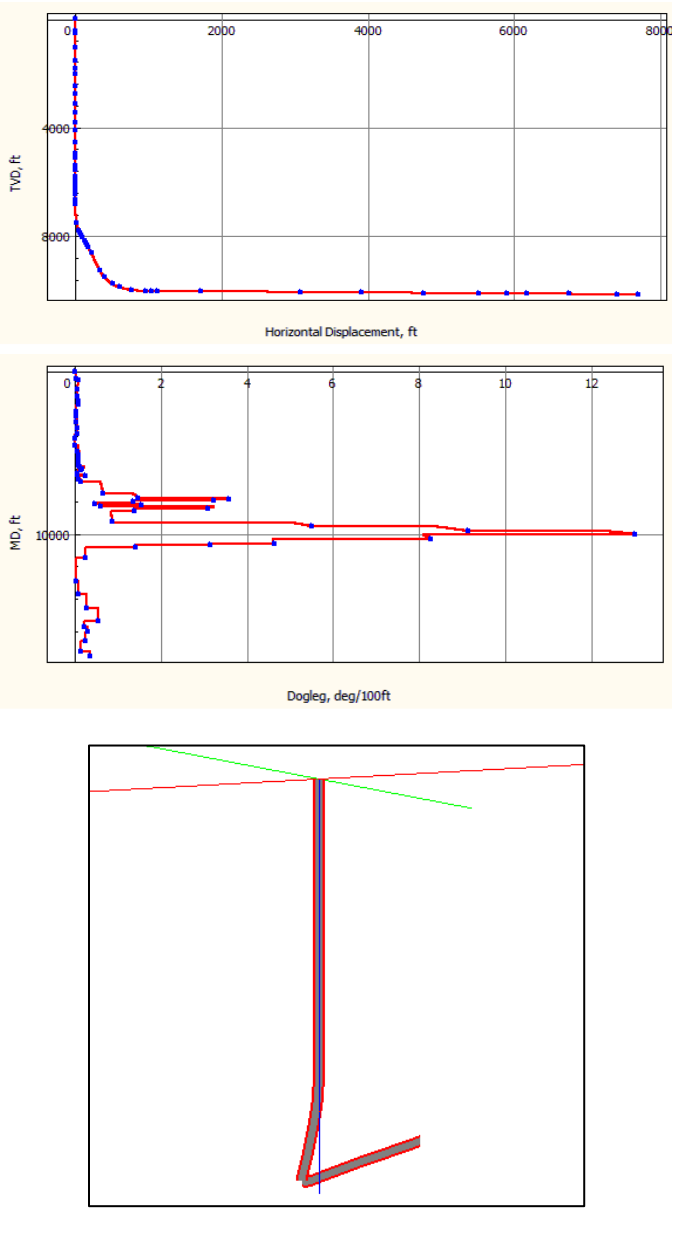

Fig. 4. Illustration of wellbore trajectory in 2D and 3D

Though our TDA model captures the main principle and relevant physics in nonlinear drilling dynamics, it still requires good quality downhole physical data to reduce the uncertainty in the prediction of dynamic response of a drilling system. For instance, the borehole diameter is not exactly the same as the size of bit but generally over-gauged and the rock specific energy varies in a wide range even for the same type of rock and it is hard to measure the real time value. The first step after model generation is usually to calibrate the model to reduce the uncertainty by comparing the model prediction with field measurement. BHA#1 was utilized to calibrate the TDA model by comparing the prediction of the lateral and axial accelerations below and above mud motor with the field measurement.

Figs. 5 and 6 show the time dependent response of the axial and lateral accelerations of BHA#1 at the locations of DDL1 and DDL2 (DDL1 indicates sensor below motor and DDL2 indicates sensor above motor). The results show that the lateral and axial acceleration vary with time, which is a good indication of the non-linear dynamic response of a drilling system. In order to be comparable with an averaged acceleration measured in the field, we utilized an root-mean-square (RMS) value to represent the magnitude of the accelerations. Both axial and lateral accelerations at the locations above and below motor are compared between model and field measurement for BHA#1. Table 1 shows the comparison of lateral and axial accelerations at locations above and below motor between TDA and field measurement. The results indicate that values of both the lateral and axial acceleration below motor are higher than those above the motor. It also shows that good comparison of accelerations are obtained with an difference less than 20%.

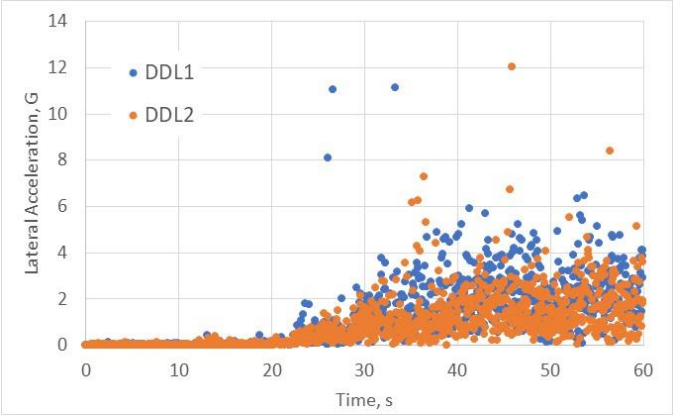

Fig. 5. Illustration of the time dependent response of axial acceleration at sensor below motor (DDL1), and sensor above motor (DDL2) for BHA#1.

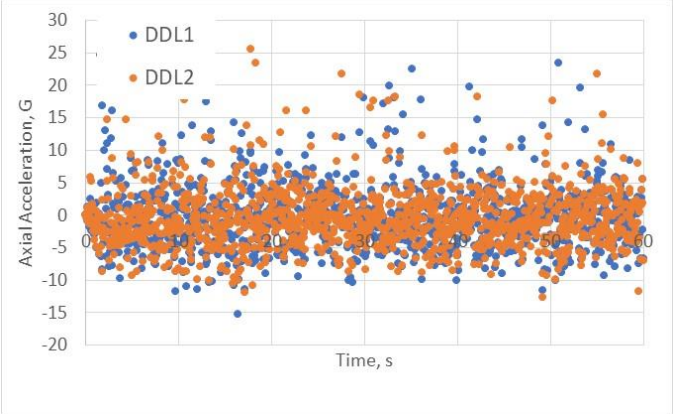

Fig. 6. Illustration of the time dependent response of lateral acceleration at sensor below motor (DDL1), and sensor above motor (DDL2) for BHA#1.

Table 1. Comparison of lateral and axial accelerations at locations above and below motor between TDA and field measurement (DDL1 indicates sensor below motor and DDL2 indicates sensor above motor).

Location	RMS of axial acceleration, G		RMS of lateral acceleration, G	
	field	TDA	field	TDA
DDL1	0.433	0.62	1.8	1.52
DDL2	0.318	0.48	0.92	0.95

After the model calibration, the nonlinear dynamic response of BHA#2 was also investigated. Fig. 7 shows the time dependent response of the lateral accelerations of BHA#2 at the location of DDL1 and DDL2. The results show that the peak lateral acceleration at DDL1 can exceed 60 G in BHA#2 while the peak lateral acceleration at DDL1 is below 20 G. The mud motor failure observed in BHA#2 might be due to the large peak lateral acceleration.

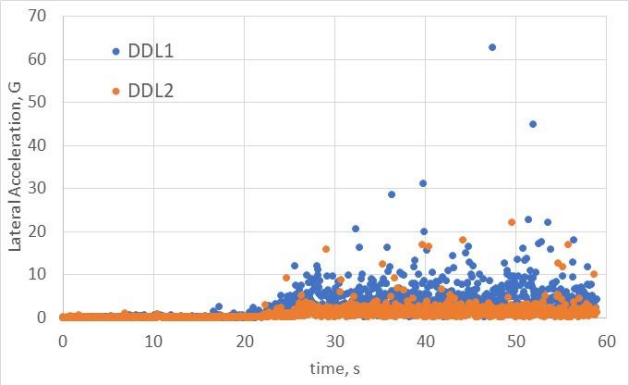

Fig. 7. Illustration of the time dependent response of axial acceleration at sensor below motor (DDL1), and sensor above motor (DDL2) for BHA#2.

Table 2 shows the comparison of lateral and axial accelerations at locations above and below motor between BHA#1 and BHA#2. The results show that higher average acceleration is observed for both axial and lateral vibrations in BHA#2. Compared to the 1/8" under gauge roller reamer, the spiral stabilizer helps to reduce the mud motor vibration significantly.

Table 2. Comparison of lateral and axial accelerations at locations above and below motor between BHA#1 and BHA#2 (DDL1 indicates sensor below motor).

Location	RMS of axial acceleration in TDA		RMS of lateral acceleration in TDA	
	BHA#1	BHA#2	BHA#1	BHA#2
DDL1	0.62	4.61	1.52	4.78
DDL2	0.48	5.11	0.95	3.12

Other than the axial and lateral acceleration, we also investigated the contact forces in the TDA. Fig. 8 shows the distribution of contact forces at static analysis, a screenshot of contact forces at TDA at the time of 40s, and the BHA deformation at the TDA at the time of 40s. The results indicate that compared to the static analysis, the contact force values and contact locations predicted in the TDA are time-dependent. In addition, the contact behavior is more complex and contact forces are higher in the TDA. As predicted in TDA, the high contact forces near the mud motor and MWD may cause failure. Other than the lateral accelerations, large contact forces predicted in TDA could probably provide insight in the tool failure.

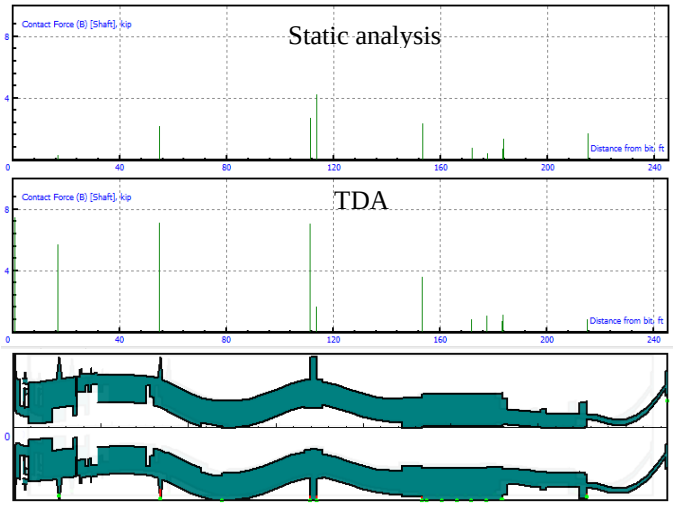

Fig. 8. Illustration of the distribution of contact forces at static analysis (top figure), contact forces at TDA (middle figure), the BHA deformation (bottom figure).

Fig. 9 illustrates the radial acceleration at the location of mud motor for BHA#2. In this figure, each dot shows the value of radial acceleration of mud motor at a certain time. The results show that the radial acceleration at the mud motor can exceed 3000 rad/s^2. The large values of radial acceleration could probably also provide insight into the mud motor failure.

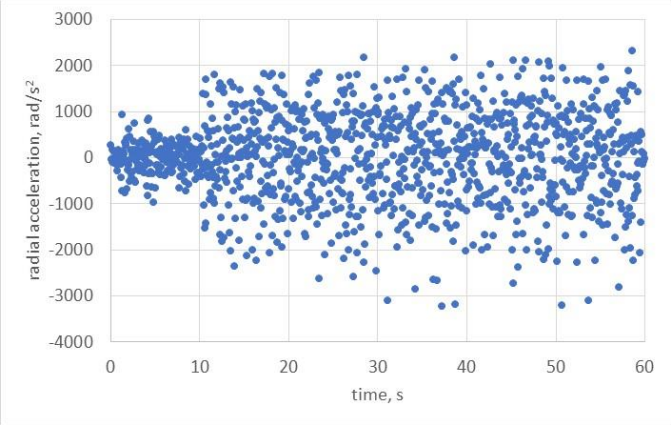

Fig. 9. Illustration of radial acceleration at the location of mud motor for BHA#2.

The TDA was also utilized to investigate the effect of full gauge reamer and under gauge reamer in the dynamic response of mud motor. Another set of the TDA has been performed for BHA#2 by replacing 1/8" under gauge roller reamer with the full gauge roller reamer. In addition, the RMS values of the axial and lateral acceleration are computed at locations above and below mud motor. Table 3 shows the Comparison of lateral and axial accelerations at locations above the below motor for BHA#2 with 1/8" under gauge roller reamer or full gauge roller reamer. The results shows that compared to 1/8" under gauge reamer, full gauge reamer induces slightly increase of axial and lateral acceleration at the location below mud motor. However, full gauge reamer induces a small drop of axial acceleration and a large drop of lateral acceleration at the location of roller reamer as the free lateral space reduces at the location of full gauge reamer.

Table 3. Comparison of lateral and axial accelerations at locations above the below motor for BHA#2 with 1/8" under gauge roller reamer or full gauge roller reamer (DDL1 indicates sensor below motor and DDL2 indicates sensor above motor).

Location	RMS of axial acceleration in TDA		RMS of lateral acceleration in TDA	
	1/8" under gauge	Full gauge	1/8" under gauge	Full gauge
DDL1	4.61	4.89	4.78	5.42
Roller reamer	5.21	4.41	1.87	1.20

Summaries

- Time domain analysis at 5520' was performed and the results are provided for BHA#1 (with stabilizer) and BHA#2 (with roller reamer).
- The acceleration of BHA#1 was first calibrated with field data at the location of DDL1 (below motor) and DDL2 (above motor).
- Compared to conventional static analysis, contact behavior in BHA is more complex at time domain analysis.
- Time varying contact force indicates shock experienced in the BHA.
- The comparison between BHA#1 and #2 shows that higher average acceleration is observed for both axial and lateral vibrations for BHA #2 and stabilizer helps to reduce both the lateral and axial vibrations.
- Compared to 1/8" under gauge roller reamer, full gauge reamer induces a large drop of lateral acceleration at the location of roller reamer.

Acknowledgments

We would like to thank MindMesh Inc. for allowing the publication.

References

1. Kamel, J.M. and Yigit, A.S. Modeling and Analysis of Stick-slip and Bit Bounce in Oil Well Drillstrings Equipped with Drag Bits. Journal of Sound and Vibration v. 333 (2014) 6885 – 6899.
2. Abedrabbo, N.E. and Line, L.A. Finite Element Simulation of Rotary Steerable Drilling Systems Advance Understanding of Damaging Downhole Shock and Vibration. Simulia Community Conference (2015).
3. Varadaraju Gandikota and Nejib Chennoufi, Improving Drilling Reliability Through Advanced Drilling Dynamics Models, Liquids-Rich Basins Conference-North America held in Midland, TX, USA, 13-14 September 2017, SPE-187487-MS
4. Dmitry Pogorelov, Gennady Mikheev & Nikolay Lysikov, Lev Ring, Raju Gandikota & Nader Abedrabbo, A Multibody System Approach to Drill String Dynamics Modeling, The ASME 2012 11th Biennial Conference on Engineering Systems Design and Analysis (ESDA2012).
5. Vadim Tikhonov, Khaydar Valiullin, Albert Nurgaleev, Lev Ring, Raju Gandikota, Pavel Chaguine, Curtis Cheatham, Dynamic Model for Stiff String Torque and Drag, 2013 SPE / IADC Drilling Conference and Exhibition, Mar 05 - 07, 2013 2013, Amsterdam, The Netherlands.
6. E. Oñate, J.M. Carbonell, C. Labra, F. Zarate, F Arrufat, L. Ring, V. Gandikota, Modeling and simulation of a rotation drilling system with drag bits using coupled discrete and finite element methods, 10th World Congress on Computational Mechanics (WCCM10), 9-13 July 2012, Sao Paolo, Brazil.
7. Vadim Tikhonov, Olga Bukashkina and Raju Gandikota, Stick-Slip Model for PDC Bits Accounting for Coupled Torsional and Axial Oscillations, ASME 2014 12th Biennial Conference on Engineering Systems Design and Analysis, Volume 2: Dynamics, Vibration and Control; Energy; Fluids Engineering; Micro and Nano Manufacturing, Copenhagen, Denmark, July 25–27, 2014.
8. Paul Pastusek, Greg Payette, Roman Shor, Eric Cayeux, Ulf Jakob Aarsnes, John Hedengren, Stéphane Menand, John Macpherson, Raju Gandikota, Michael Behounek, Richard Harmer, Emmanuel Detournay, Roland Illerhaus, Yu Liu. Creating Open Source Models, Test Cases, and Data for Oilfield Drilling Challenges. 2019 SPE / IADC Drilling Conference and Exhibition, Mar 05 - 07, 2019, Hague, The Netherlands.